Development of a Semiautomated Zero Length Column Technique for Carbon Capture Applications

Development of a Semi-Automated Zero Length Column Technique for Carbon Capture Applications: Study of Diffusion Behaviour of CO_2 in MOFs

Xiayi Hu[1*], *Stefano Brandani*[1†], *Annabelle I. Benin*[2] *and Richard R. Willis*[2]

1. Institute for Materials and Processes, School of Engineering, the University of Edinburgh, UK

2. New Materials Research, UOP LLC, a Honeywell Company, Des Plaines, IL, USA

† Corresponding author.

* Current address:
College of Chemical Engineering, Xiangtan University, Hunan Province, 411105, P. R. China

Email address: s.brandani@ed.ac.uk

ABSTRACT

A semi-automated zero length column (ZLC) technique has been applied to investigate diffusion behaviour of CO_2 in metal organic framework Co/DOBDC powder and in Ni/DOBDC pellets. For Co/DOBDC crystals, since the system was close to equilibrium control even at the highest flow rate achievable in the ZLC, a lower limit of the micropore diffusivity was estimated, which indicates that for this MOF topology in conditions that are characteristic of practical carbon capture applications the process would be macropore diffusion controlled. This was confirmed on formed samples of Ni/DOBDC pellets for which experimental proof of the prevailing mass transfer resistance was obtained by performing ZLC experiments with different carrier gases. The kinetic experiments were used to determine void fraction and tortuosity values for the pellets.

Key words: Zero length column (ZLC), adsorption, MOFs, CO_2 capture, kinetics

INTRODUCTION

Recently, metal−organic frameworks (MOFs) have attracted a great deal of attention as a new class of microporous materials.[1-5] The unique structure of MOFs makes them attractive as adsorbents for CO_2 adsorption with properties that are better than other porous materials, such as silicates, carbons, and zeolites.[6, 7] This has the potential for making a significant impact in CO_2 capture from flue gas since some of the MOFs offer high capacity even at low CO_2 partial pressure.[8-12] For example, DOBDC MOFs (M_2(dhtp), dhtp = 2,5-dihydroxyterephthalate) consist of a three-dimensional honeycomb lattice with one-dimensional pores (diameter ~ 12 Å). The benzenedicarboxylates ligands linked with the metal clusters via an oxygen atom, these types of MOFs show comparable CO_2 capture capacity with amine.[9, 10, 12-15]

For the optimal design and operation of commercial CO_2 capture processes, in addition to equilibrium properties, it is important to investigate the rates of CO_2 adsorption. Experimental research on diffusion of gases including CO_2 in MOFs is limited in the literature. Zhao et al.[16] measured the diffusion coefficient of CO_2 in MOF-5 (cage with cavity of 12 Å and aperture opening of 8 Å) to be in the range of $8.1-11.5 \times 10^{-13}$ m^2/s at 295−331K with an activation energy of 7.61 kJ/mol. Saha et al.[17] investigated the average diffusivity of CO_2 in MOF-177 and found it to be in the order of 10^{-9} m^2/s at 298 K using a Micromeritics ASAP 2020 adsorption unit. Sabouni et al.[18] studied the kinetics of CO_2 adsorption on CPM-5 samples volumetrically in the pressure range of 5–105 kPa by means of a Micromertics ASAP 2010 using the ROA software and obtained a value of 1.86×10^{-12} m^2/s,

7.04×10^{-12} m^2/s, and 7.87×10^{-12} m^2/s at 273 K, 298 K and 318 K, respectively. Jian et al.[19] studied CO_2 adsorption rates from helium for HKUST-1 and Ni/DOBDC pellets using a unique concentration-swing frequency response (CSFR) system. Mass transfer into the MOFs is rapid with the controlling resistance found to be macropore diffusion. Other research is focused on theoretical and simulation work[20, 21], therefore, it is quite important to develop a system for measuring kinetics of novel adsorbents for carbon dioxide capture.

The Zero Length Column (ZLC) is a chromatographic technique which was invented for diffusivity measurements of pure gases on microporous solids.[22] The advantage of this method is the elimination of external mass and heat transfer resistances by the use of low adsorbate concentrations, very small adsorbent sample amounts, as well as high carrier flow rates during desorption. It has been extensively used for diffusivity measurements in zeolites and for measuring the diffusion in biporous materials.[23-26] In our part-1 of this study we described the development of a semi-automatic ZLC system and demonstrated its use in screening novel CO_2 adsorbents based on equilibrium capacities using less than 15 mg of sample. Of the MOFs investigated, the M-DOBDC (with M = Mg; Ni; and Co) showed significant potential in terms of CO_2 adsorption capacity. In this work, the new semi-automated ZLC system has been applied to investigate the diffusion behaviour of CO_2 in DOBDC MOFs.

THEORY

The ZLC technique is based on the concept that as the column length decreases the system becomes equivalent to a perfectly mixed cell. The column mass balance is then given by

$$V_s \frac{d\bar{q}}{dt} + V_g \frac{dc}{dt} + Fc = 0 \qquad (1)$$

where the mass balance for a biporous spherical particle is given by[27] the mass balance in the macropores

$$(1-\varepsilon_P)\frac{\partial \bar{n}}{\partial t} + \varepsilon_P \frac{\partial c_P}{\partial t} = \frac{\varepsilon_P}{\tau} D_{Macro}\left(\frac{\partial^2 c_P}{\partial R^2} + \frac{2}{R}\frac{\partial c_P}{\partial R}\right) \qquad (2)$$

and the mass balance in the micropores

$$\frac{\partial n}{\partial t} = D_{Micro}\left(\frac{\partial^2 n}{\partial r^2} + \frac{2}{r}\frac{\partial n}{\partial r}\right) \qquad (3)$$

where

$$\frac{\partial \bar{n}}{\partial t} = \frac{3}{r_C} D_{Micro} \left.\frac{\partial n}{\partial r}\right|_{r=r_C} \qquad (4)$$

and

$$\frac{\partial \bar{q}}{\partial t} = \frac{3}{R_P}\frac{\varepsilon_P}{\tau} D_{Macro} \left.\frac{\partial c_P}{\partial R}\right|_{R=R_P} \qquad (5)$$

Even when the solid is bi-porous in most cases only one mass transfer resistance controls the kinetics. The micropore diffusional time constant is r_C^2/D_{Micro}. This should be compared to the effective macropore diffusional time constant which is obtained from Eq. 2 if one assumes that the adsorbate in the micropores is at equilibrium with the fluid concentration in the macropores. In this case, assuming linear equilibrium, $\bar{n} = Hc_P$, we can write[27]

$$\left[(1-\varepsilon_P)H + \varepsilon_P\right]\frac{\partial c_P}{\partial t} = \frac{\varepsilon_P}{\tau} D_{Macro}\left(\frac{\partial^2 c_P}{\partial R^2} + \frac{2}{R}\frac{\partial c_P}{\partial R}\right) \qquad (6)$$

We note that at the conditions typical of ZLC experiments carried out in this study, D_{Macro} corresponds primarily the bulk gas diffusivity of the adsorbate molecules in the carrier gas which can be estimated from known correlations.[28]

From Eq 6, the effective macropore diffusivity is defined by

$$D_{Eff} = \frac{\varepsilon_P}{\tau} \frac{D_{Macro}}{[(1-\varepsilon_P)H + \varepsilon_P]} \tag{7}$$

and the macropore diffusional time constant is R_P^2 / D_{Eff}. The ratio of the two time constants provides an indication of which one is slower and hence is controlling mass transfer.

$$\frac{D_{Eff}}{R_P^2} \frac{r_C^2}{D_{Micro}} = \frac{r_C^2}{R_P^2} \frac{\varepsilon_P}{\tau} \frac{D_{Macro}/D_{Micro}}{[(1-\varepsilon_P)H + \varepsilon_P]} \tag{8}$$

Since beads or pellets are typically of the order of a mm in diameter and crystals are in the range of microns and given that the dimensionless Henry law constant can be greater than 10^2-10^3, only microporous solids with channel sizes that are very close to the dimension of the molecule diffusing in the system will be micropore diffusion controlled.

M-DOBDC MOFs have 12 Å channels, therefore one would expect to see macropore diffusion control, and the effective diffusivities for CO_2 should be in the inverse order of the adsorption capacities, ie Co > Ni > Mg. For this reason and for the fact that Co-DOBDC could be synthesised to obtain the largest crystals, ZLC measurements were carried out on Co-DOBDC powders first to obtain an estimate of D_{Micro} and experiments on Ni-DOBDC pellets (which are stable in water) were used to confirm the controlling mass transfer mechanism.

If in the solid only one mass transfer resistance is controlling then for a linear adsorption isotherm the solution to the diffusion model yields[27, 29]

$$\frac{c}{c_0} = 2L\sum_{n=1}^{\infty}\frac{exp(-\beta_n{}^2 Dt/R^2)}{[\beta_n{}^2 + \left(L-1-\gamma\beta_n{}^2\right)^2 + L-1+\gamma\beta_n{}^2]} \qquad (9)$$

where β_n are the positive roots of:

$$\beta_n \cot\beta_n + L - 1 - \gamma\beta_n^2 = 0 \qquad (10)$$

and

$$\gamma = \frac{V_g}{3KV_s} \qquad (11)$$

$$L = \frac{1}{3}\frac{F}{KV_s}\frac{R^2}{D} \qquad (12)$$

For powders, ie no macropore structure

$$K = H \quad ; \qquad \frac{D}{R^2} = \frac{D_{Micro}}{r_C^2} \qquad (13)$$

For biporous solids under macropore diffusion control[27]

$$K = \varepsilon_P + (1-\varepsilon_P)H \quad ; \qquad \frac{D}{R^2} = \frac{D_{Eff}}{R_P^2} \qquad (14)$$

To achieve kinetic control in ZLC experiments it is necessary to achieve high values of the parameter L. This is obtained by increasing the flowrate, F, and reducing the sample mass, ie reducing the solid volume V_s.

EXPERIMENTAL

Co/DOBDC Powder

Co/DOBDC was synthesized through solvothermal reactions modified from the literature. [13] The reaction of cobalt (II) acetate and 2, 5-dihydroxyterephthalic acid ($C_8H_6O_6$) in a mixture of water and tetrahydrofuran (molar ratio 2:1:556:165) under autogenous pressure at 110 °C in a Teflon-lined autoclave (50% filling level). This yielded pink-red, needle-shaped crystals of $[Co_2\ (C_8H_2O_6)(H_2O)_2]8H_2O$ (Figure 1). After the hypothetical removal of the non-coordinating solvent molecules in the channels, the empty channels occupy 49% of the total volume of the unit cell, and the average cross-sectional channel dimensions are 11.08×11.08 $Å^2$. The empty volume increases to 60% if the coordinating water is also removed. The water molecules excluding and including the coordinating water account for 29.2% and 36.6% of the mass, respectively. The BET surface area for this sample was found to be 957 m^2/g. The Co/DOBDC adsorbent had the largest crystal size of all the crystals that were synthesised and supplied by UOP. The SEM image is shown in Figure 1.

About three mg of Co/DOBDC powder was packed between two porous stainless steel sinter discs held in one end of a Swagelok 1/8 in. union. Prior to the experiment, the sample was regenerated with a ramping rate of 1°C/min to 125°C and then held at this temperature for 12h at 1 cc/min of helium purge. After regeneration, the oven temperature was reduced to 38°C and the flow system switched to the high flowrate mass flow controllers (MFCs). This was to provide conditions for the ZLC desorption

process controlled by kinetics (high L value) and is the reason to include two sets of MFCs in the system. During an experiment, the sample was first equilibrated with a helium stream containing 10% of CO_2 which was prepared in the dosing volume. At time zero, the flow was switched to a pure helium purge stream at the same flow rate. The sorbate concentration at the outlet of the ZLC can be conveniently followed using a mass spectrometer (MS). ZLC experiments were carried out at two different flow rates (at 30 and 45 cc/min) in order to establish kinetic or equilibrium control.

Ni/DOBDC pellets

Ni/DOBDC is synthesized through solvothermal reactions modified from the literature. [13] Nickel(II) acetate (18.7 g, 94.0 mmol, Aldrich) and 2,5-dihydroxyterephthalic acid (DOBDC, 37.3 g, 150 mmol, Aldrich) were placed in 1 L of mixed solvent consisting of equal parts tetrahydrofuran (THF) and deionized water. The mixture was then put into a 2 L static Parr reactor and heated at 110 °C for 3 days. The as-synthesized sample was filtered and washed with water. Then the sample was dried in air, and the solvent remaining inside the sample was exchanged with ethanol 6 times over 8 days. Finally, the sample was activated at 150°C under vacuum with nitrogen flow. The BET surface area for the powder sample was found to be 936 m^2/g.

Figure 2 (a) shows the pressed Ni/DBODC pellet which does not contain a binder. Since the ZLC is packed in a 1/8" Swagelok union fitting, the original pellet could not

be tested directly. Fragments of different sizes were broken off the material as shown in

Figure 2 (b), (c) and (d).

Prior to the experiment, the sample was thermally regenerated with a ramping rate of 1 °C/min to 150 °C and then held this temperature for 12h at 1 cc/min of the helium purge gas. After regeneration, the oven temperature is reduced to 38 °C and the flow system switched to high flowrate mass flow controllers. During an experiment, the sample was first equilibrated with inert stream containing 10% of CO_2. At time zero, the flow was switched to a pure helium purge stream at the same flow rate. For each sample, ZLC experiment runs at different flow rates were performed in the range of 5 - 45 cc/min.

If the system is under macropore diffusion control it is possible to verify this conveniently using different purge gases (He and N_2) which result in different molecular diffusivities. Different bead sizes can also be used and given that the experiment is carried out on a single bead this introduces a small uncertainty due to the variable void fraction and tortuosity.

If the mass transfer rate is controlled by intracrystalline diffusion, desorption curves measured under similar conditions with different purge gases, should be identical.[28]

RESULTS AND DISCUSSION

Co/DOBDC Powder

The dimensions of the crystals were measured using the image analysis tool GIMP on 176 crystals. While the crystals considered are more similar to 3D bodies with square or rectangular faces, for mass transfer purposes the kinetics can be approximated by the behaviour of spheres that have the same surface to volume ratio = $3/R_c$.[30] The crystal dimensions are converted to an equivalent radius using a size interval of 1 μm. The resulting log-normal distribution (PSD) (log-normal distribution of the numbers of crystals in each size interval) is examined to determine the mean crystal diameter. In Figure 3, a log-normal of distribution curve is plotted. From the log-normal probability curve, the mean diameter was found to be approximately 6.5 μm.

The traditional analysis of ZLC curves[22] neglects the effect of particle size distributions. Duncan and Moller[24] studied the effect of size distribution in ZLC experiments in detail. They found that analysing such a curve with the standard ZLC model and the long-time asymptote causes the diffusional time constant to be under-predicted, whereas the adsorption related parameter (L) is over-predicted, and that the error increases with increasing distribution width. This can be understood qualitatively since the long-time asymptote will correspond to the largest crystals, while the diffusivity is extracted using the mean diameter. While this could be important for the accurate determination of the micropore diffusivity, since the system

is always under equilibrium control it is still possible to estimate a lower bound on the diffusivity which is independent of the fact that the crystals are not of uniform size.

For an accurate interpretation of ZLC data, it is essential to check whether the overall kinetics of desorption, as measured by the ZLC, is controlled by kinetics or by equilibrium. One way of checking this condition is by plotting ln (c/c_o) vs. Ft (flowrate times time). For equilibrium-controlled processes, the response curves should be independent of flowrate in this plot, implying an overlap of curves, whereas the curves diverge for a kinetically controlled process. The ZLC desorption curve and the experimental Ft plots for Co/DODBDC crystals are shown in Figure 4 and Figure 5.

The results of the Ft plots (Figures 4 and 5) indicate that the curves overlap, so the system is still under equilibrium control even at the highest flow rate. For a CO_2 capture process, this is actually a positive result, since in an equilibrium-driven processes mass transfer limitations reduce the separation efficiency of the material.

To estimate a lower bound on the micropore diffusivity we consider that equilibrium control indicates that the L parameter is less than 1. From the definition of L, Eq. 12, the maximum flowrate and the equilibrium constant it is possible to conclude that the diffusivity is greater than $2x10^{-12}$ m^2/s.

Ni/DOBDC Pellets

For mass transfer purposes, the images in Figure 2 were used to obtain an effective radius which gives the same surface to volume ratio. Table 1 includes the dimensions measured by the image analysis tool GIMP of the individual pellets and the equivalent radius calculated on this basis.

Figure 6 shows a qualitative comparison of the CO_2 adsorption capacity for the different Ni-DOBDC fragments (R = 0.57 mm, R = 0.79 mm, or R = 1.19 mm) at 0.1bar of CO_2 in helium, 38 °C, 5 cc/min versus the blank response. This initial test was carried out to check if these fragments showed consistent adsorption capacities. It is quite clear that there is very little variation in adsorption capacity between the three fragments.

The experimental Ft plots for the Ni/DOBDC pellets of particle size 0.57mm, 0.79 mm and 1.19 mm are shown in Figures 7-9 (10% CO_2 in helium, 38ºC, Flowrate = 5,10, 20, 30 and 45 cc/min), respectively. As shown in Figure 7, the representative response curves for the smallest pellets (R = 0.57 mm) at five different purge rates are clearly overlapping, confirming that the process is close to equilibrium control because of the low R value. On the other hand, the Ft plots from the other two pellets (R = 0.79 mm, R = 1.19 mm) clearly indicate that the desorption is kinetically controlled.

The ZLC desorption curve of the pellets (R = 0.79 mm and 1.19 mm at 38 °C) are shown in Figure 10 and Figure 11, respectively. Based on the blank response, it is clear that the system baselined after 3 seconds, but there is a drift when concentration is lower than 0.05. Therefore to obtain a reliable diffusivity value without a systematic error, the slope of the long time asymptote was selected in-between the concentrations from 0.1 to 0.05. The diffusional time constants can be estimated clearly from the plots, since the desorption curves of the three highest flowrates (20, 30 and 45 cc/min) are nearly parallel to each other, in conformity with the kinetic control limit.

From the results on Co/DOBDC crystals we assumed that the micropore diffusivity in similar materials is at least 10^{-12} m^2/s. This means that for a 1 μm crystal the corresponding micropore diffusional time constant (R^2/D) should be less than 1s. The kinetic response observed on Ni/DOBDC pellet is clearly much slower than this. The diffusional time constant obtained from the ZLC desorption curves allows a direct comparison between the two pellet sizes, i.e. 0.022/0.009 = 2.4 can be compared directly with $(1.19/0.79)^2 = 2.3$. This shows that within the experimental uncertainty the data are consistent with macropore diffusion control.

To validate further the assumption that the Ni/DOBDC pellet is under macropore diffusion control additional experiments using different purge gases (He and N_2) were

performed. If the mass transfer rate is controlled by micropore diffusion desorption curves measured under similar conditions with different purge gas should be identical.[22] The experiments were repeated on the largest pellet (R = 1.19 mm) using N_2 as the purge gas under the same conditions. Figure 12 shows that the Ft plot confirmed kinetic control on the pellet (divergent curves). Figure 13 shows the comparison of the replicate desorption curves obtained with helium and nitrogen purge gas. It can be seen that desorption curves are dependent on the purge gas providing further experimental confirmation of macropore diffusion control.

Combining the results at low flowrates, which yield an accurate estimate of K, and those at high flowrates which give and accurate estimate of D_{Eff}/R_P^2 it is possible to decouple the diffusivity from the equilibrium constant and obtain $\frac{\varepsilon_P}{\tau} D_{Macro}$. If the further assumption that the diffusion is given by a random walk around fixed objects is made, then the approximation $\tau = \frac{1}{\varepsilon_P}$ can be used to estimate the void fraction and tortuosity of the pellets.[31] The values obtained are included in Table 2 and show that the resulting parameters are physically meaningful.[30]

CONCLUSIONS

For the detailed design of carbon capture processes based on MOF adsorbents it is necessary to determine both equilibrium and kinetic parameters. The results presented clearly show that for the M-DOBDC class of materials under conditions typical of

carbon capture applications the system is macropore diffusion controlled. This has been validated by a series of experiments on both powders and pellets.

For the largest crystals available (Co-DOBDC) a lower bound on the micropore diffusivity was found to be $2x10^{-12}$ m^2/s, which corresponds to a diffusional time constant of approximately 1 s for typical crystals of 1 μm. Since Co-DOBDC has the smallest CO_2 capacity this indicates that for both Ni- and Mg-DOBDC macropore diffusion control is to be expected as the controlling mass transfer resistance.

Experiments on fragments of a pellet of Ni-DOBDC were used to confirm the controlling mechanism. The high flowrate mass flow controllers on the semi-automated ZLC system achieved flowrates which were sufficiently high to be under kinetic control conditions. The macropore diffusion control was confirmed both by comparing fragments of different sizes and by repeating the experiments with different carrier gases.

The methodology presented has demonstrated the effectiveness of a properly designed ZLC system in determining both equilibrium and kinetic parameters for carbon capture applications.

ACKNOWLEDGEMENTS

This project was supported by the U.S. Department of Energy through the National Energy Technology Laboratory under Award No. DE-FC26-07NT43092. However, any opinions, findings, conclusions, or recommendations expressed herein are those of the authors and do not necessarily reflect the views of the DOE.

REFERENCES

(1) Panella, B.; Hirscher, M.; Pütter, H.; Müller, U. Hydrogen Adsorption in Metal–Organic Frameworks: Cu-MOFs and Zn-MOFs Compared. *Adv. Funct. Mater.* **2006**, 16, 520-524.

(2) Rowsell, J. L. C.; Millward, A. R.; Park, K. S.; Yaghi, O. M. Hydrogen Sorption in Functionalized Metal Organic Frameworks. *J. Am. Chem. Soc.* **2004**, 126, 5666-5667.

(3) Furukawa, H.; Ko, N.; Go, Y. B.; Aratani, N.; Choi, S. B.; Choi, E.; Yazaydin, A. Ö.; Snurr, R. Q.; O'Keeffe, M.; Kim, J.; Yaghi, O. M. Ultrahigh Porosity in Metal-Organic Frameworks. *Science* **2010**, 329, 424-428.

(4) Wilmer, C. E.; Leaf, M.; Lee, C. Y.; Farha, O. K.; Hauser, B. G.; Hupp, J. T.; Snurr, R. Q. Large-scale screening of hypothetical metal–organic frameworks. *Nat. Chem.* **2012**, 4, 83-89.

(5) Wilmer, C. E.; Farha, O. K.; Yildirim, T.; Eryazici, I.; Krungleviciute, V.; Sarjeant, A. A.; Snurr, R. Q.; Hupp, J. T. Gram-scale, high-yield synthesis of a robust metal-organic framework for storing methane and other gases. *Energy Environ. Sci.* **2013**, 6, 1158-1163.

(6) Millward, A. R.; Yaghi, O. M. Metal Organic Frameworks with Exceptionally High Capacity for Storage of Carbon Dioxide at Room Temperature. *J. Am. Chem. Soc.***2005**, 127, 17998-17999.

(7) Xiang, S. C.; He, Y. B.; Zhang, Z. J.; Wu, H.; Zhou, W.; Krishna, R.; Chen, B. L. Microporous metal-organic framework with potential for carbon dioxide capture at ambient conditions. *Nat. Commun.* **2012**, 3, No. 954.

(8) Chen, B.; Ockwig, N. W.; Millward, A. R.; Contreras, D. S.; Yaghi, O. M. High H2 Adsorption in a Microporous Metal–Organic Framework with Open Metal Sites. *Angew. Chem. Int. Ed.***2005**, 44, 4745-4749.

(9) Caskey, S. R.; Wong-Foy, A. G.; Matzger, A. J. Dramatic Tuning of Carbon Dioxide Uptake via Metal Substitution in a Coordination Polymer with Cylindrical Pores. *J. Am. Chem. Soc.* **2008**, 130, 10870-10871.

(10) Yazaydin, A. O.; Benin, A. I.; Faheem, S. A.; Jakubczak, P.; Low, J. J.; Willis, R. R.; Snurr, R. Q. Enhanced CO_2 Adsorption in Metal-Organic Frameworks via Occupation of Open-Metal Sites by Coordinated Water Molecules. *Chem. Mater.* **2009**, 21, 1425-1430.

(11) Yazaydin, A. O.; Snurr, R. Q.; Park, T.-H.; Koh, K.; Liu, J.; LeVan, M. D.; Benin, A. I.; Jakubczak, P.; Lanuza, M.; Galloway, D. B.; Low, J. J.; Willis, R. R. Screening of Metal-Organic Frameworks for Carbon Dioxide Capture from Flue Gas Using a Combined Experimental and Modeling Approach. *J. Am. Chem. Soc.* **2009**, 131, 18198-18199.

(12) Remy, T.; Peter, S. A.; Van der Perre, S.; Valvekens, P.; De Vos, D. E.; Baron, G. V.; Denayer, J. F. M. Selective Dynamic CO_2 Separations on Mg-MOF-74 at Low Pressures: A Detailed Comparison with 13X. *J. Phys. Chem. C* **2013**, 117, 9301-9310.

(13) Rosi, N. L.; Kim, J.; Eddaoudi, M.; Chen, B.; O'Keeffe, M.; Yaghi, O. M. Rod Packings and Metal-Organic Frameworks Constructed from Rod-Shaped Secondary Building Units. *J. Am. Chem. Soc.* **2005**, 127, 1504-1518.
(14) Low, J. J.; Benin, A. I.; Jakubczak, P.; Abrahamian, J. F.; Faheem, S. A.; Willis, R. R. Virtual High Throughput Screening Confirmed Experimentally: Porous Coordination Polymer Hydration. *J. Am. Chem. Soc.* **2009**, 131, 15834-15842.
(15) Li, W.; Bollini, P.; Didas, S. A.; Choi, S.; Drese, J. H.; Jones, C. W. Structural Changes of Silica Mesocellular Foam Supported Amine-Functionalized CO_2 Adsorbents Upon Exposure to Steam. *ACS Appl. Mater. Inter.* **2010**, 2, 3363-3372.
(16) Zhao, Z.; Li, Z.; Lin, Y. S. Adsorption and Diffusion of Carbon Dioxide on Metal Organic Framework (MOF-5). *Ind. Eng. Chem. Res.* **2009**, 48, 10015-10020.
(17) Saha, D.; Bao, Z.; Jia, F.; Deng, S. Adsorption of CO_2, CH_4, N_2O, and N_2 on MOF-5, MOF-177, and Zeolite 5A. *Environ. Sci. Technol.* **2010**, 44, 1820-1826.
(18) Sabouni, R.; Kazemian, H.; Rohani, S. Carbon dioxide adsorption in microwave-synthesized metal organic framework CPM-5: Equilibrium and kinetics study. *Microporous Mesoporous Mat.* **2013**, 175, 85-91.
(19) Liu, J.; Wang, Y.; Benin, A. I.; Jakubczak, P.; Willis, R. R.; LeVan, M. D. CO_2/H_2O Adsorption Equilibrium and Rates on Metal Organic Frameworks: HKUST-1 and Ni/DOBDC. *Langmuir* **2010**, 26, 14301-14307.
(20) Skoulidas, A. I. Molecular Dynamics Simulations of Gas Diffusion in Metal Organic Frameworks:Argon in CuBTC. *J. Am. Chem. Soc.* **2004**, 126, 1356-1357.
(21) Babarao, R.; Jiang, J. Diffusion and Separation of CO_2 and CH_4 in Silicalite, C168 Schwarzite, and IRMOF-1: A Comparative Study from Molecular Dynamics Simulation. *Langmuir* **2008**, 24, 5474-5484.
(22) Eic, M.; Ruthven, D. M. A new experimental technique for measurement of intracrystalline diffusivity. *Zeolites* **1988**, 8, 40-45.
(23) Brandani, S.; Ruthven, D. M. Analysis of ZLC desorption curves for gaseous systems. *Adsorption* **1996**, 2,133-143.
(24) Duncan, W. L.; Moller, K. P. The effect of a crystal size distribution on ZLC experiments. *Chem. Eng. Sci.* **2002**, 57, 2641-2652.
(25) Brandani, F.; Ruthven, D.; Coe, C. G. Measurement of Adsorption Equilibrium by the Zero Length Column (ZLC) Technique Part 1:Single-Component Systems. *Ind. Eng. Chem. Res.* **2003**, 42, 1451-1461.
(26) Ruthven, D. M.; Xu, Z. Diffusion of oxygen and nitrogen in 5A zeolite crystals and commercial 5A pellets. *Chem. Eng. Sci.* **1993**, 48, 3307-3312.
(27) Brandani, S. Analytical solution for ZLC desorption curves with bi-porous adsorbent particles. *Chem. Eng. Sci.***1996**, 51, 3283-3288.
(28) Bird, R. B.; Stewart, W. E.; Lightfoot, E. N., *Transport Phenomena* 2nd Ed. ed.; Wiley: New York, 2002.
(29) Brandani, S.; Ruthven, D. M. Analysis of ZLC desorption curves for liquid systems. *Chem. Eng. Sci.* **1995**, 50, 2055-2059.
(30) Ruthven, D. M., *Principles of Adsorption and Adsorption Processes*. Wiley: New York, 1984.

(31) Gibilaro, L. G., *Fluidization Dynamics*, Ed. Butterworth-Heinemann: Oxford, 2001.

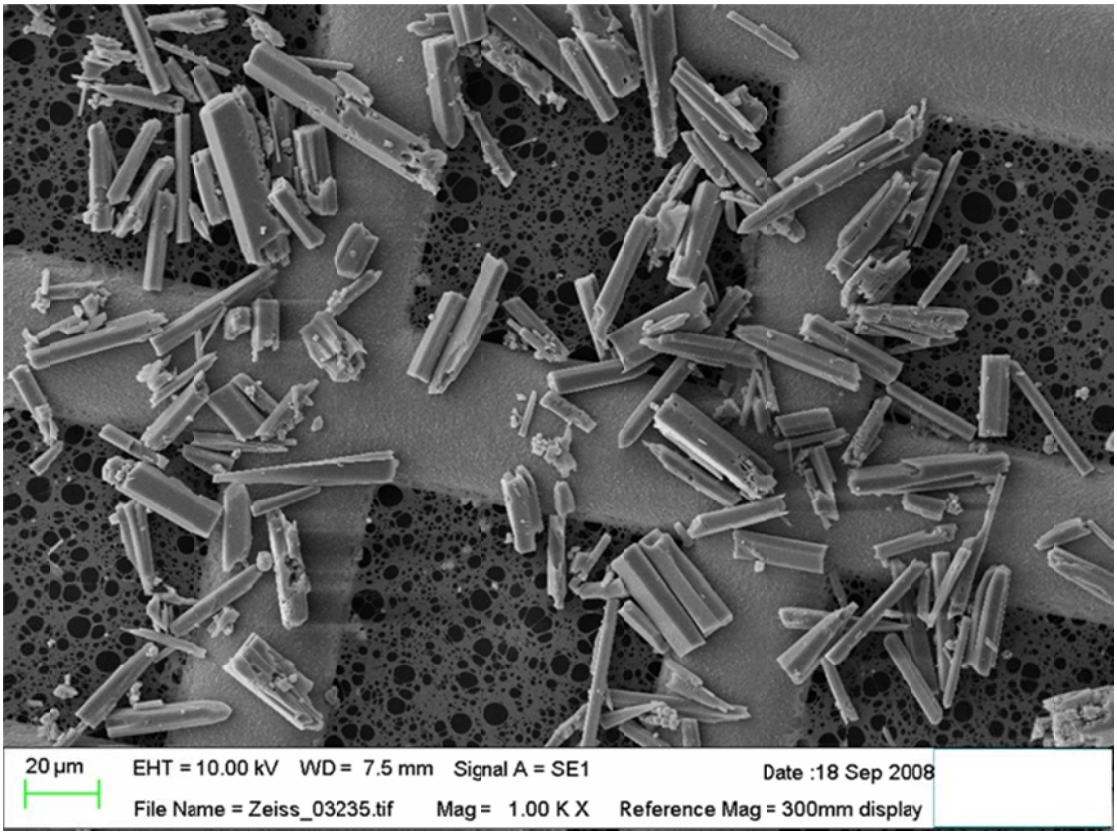

Figure 1. SEM image of Co/DOBDC crystals.

(a)

(b)

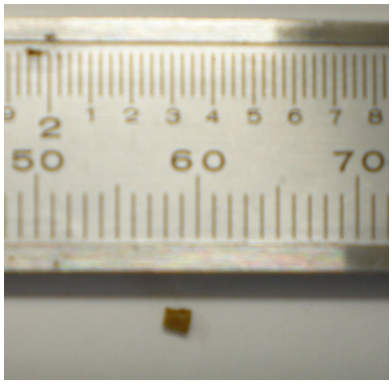

(c)

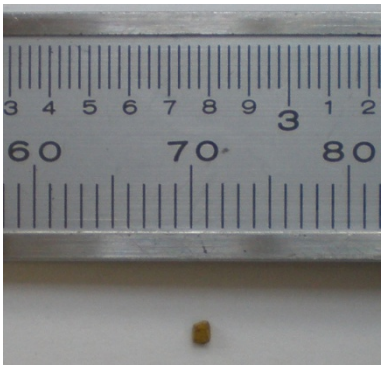

(d)

Figure 2. Formed pellet and fragments used in the kinetic experiments. (a) Original pellet; (b) 1.19 mm fragment; (c) 0.79 mm fragment; (d) 0.57 mm fragment.

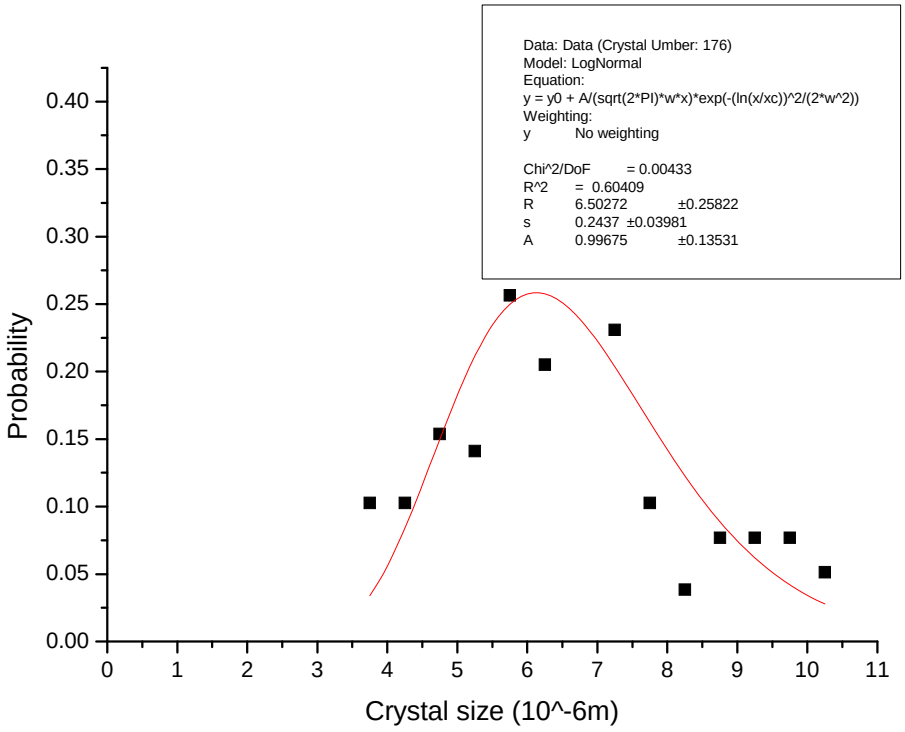

Figure 3. Size distribution of Co/DOBDC crystals.

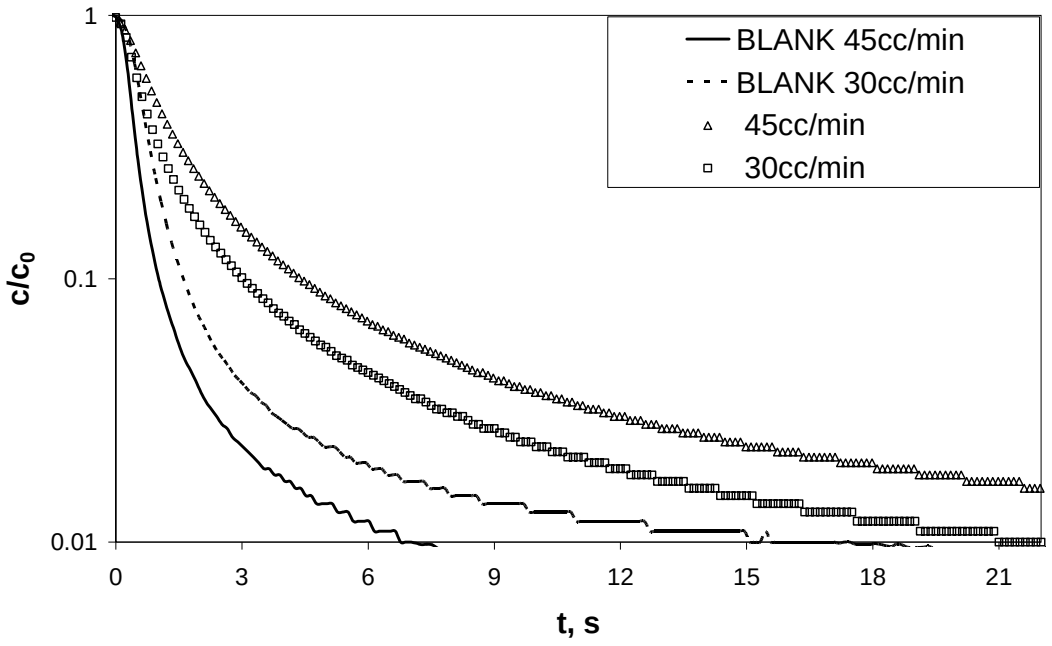

Figure 4. ZLC curves for Co/DOBDC at 30 and 45 cc/min at 38 °C.

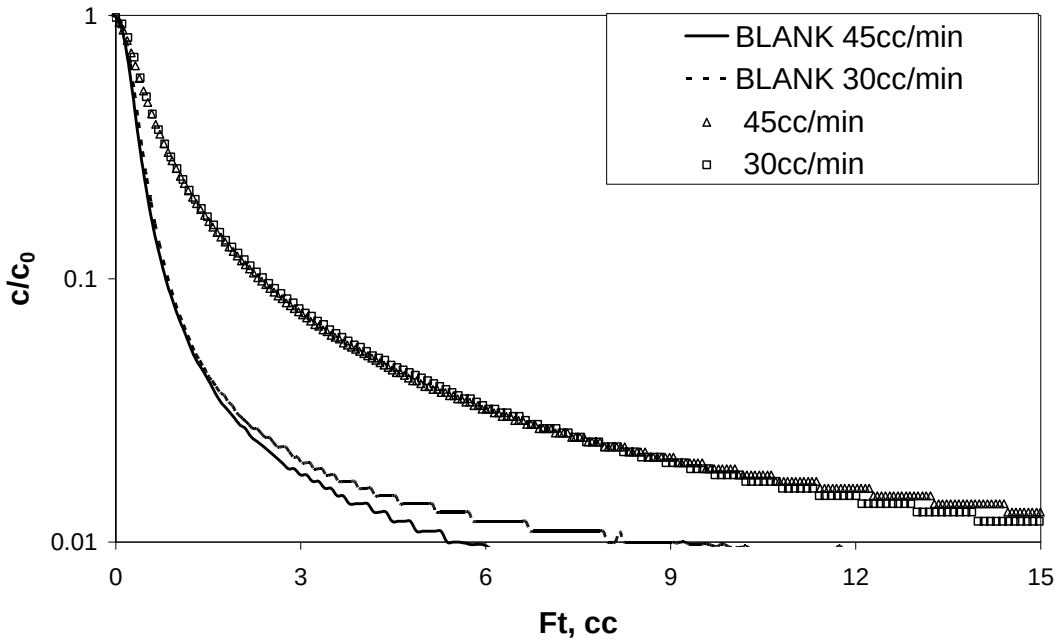

Figure 5. ZLC curves for Co/DOBDC at 30 and 45 cc/min at 38 °C.

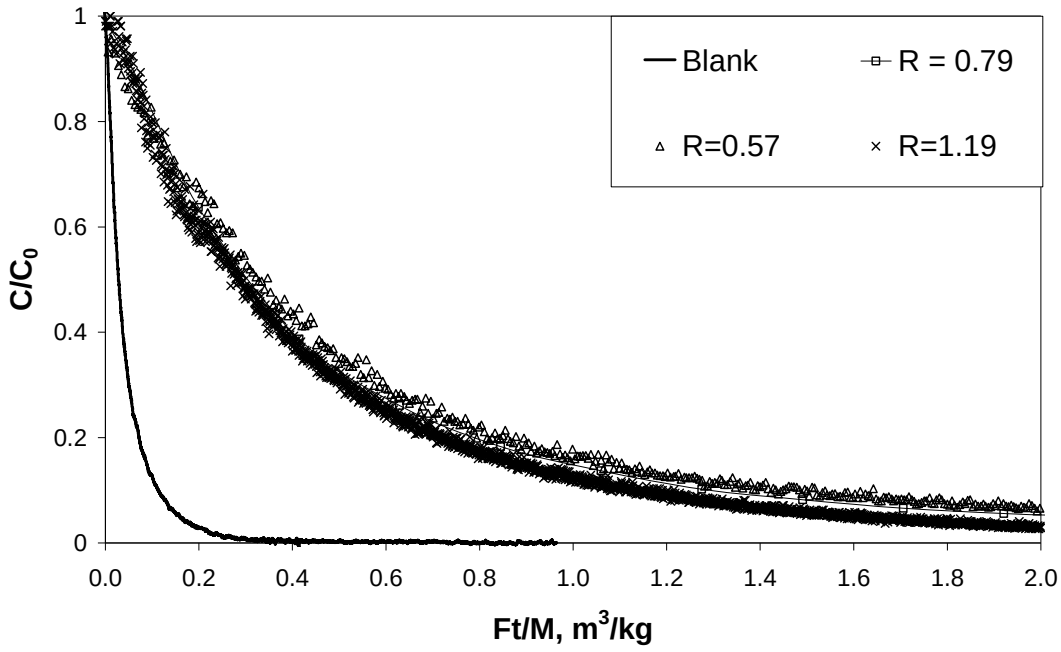

Figure 6. Comparison of adsorbent capacity of different Ni/DOBDC fragments. (R = 0.57 mm, R = 0.79 mm, R = 1.19 mm) at 0.1bar of CO_2 in helium, 38 °C, 5 cc/min and the blank response.

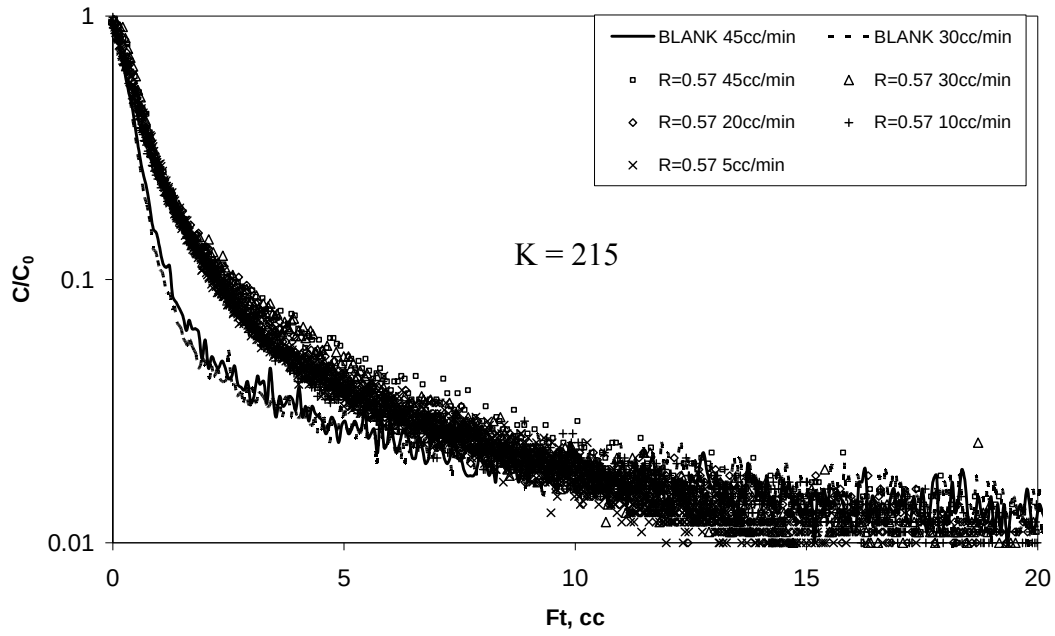

Figure 7. Experimental Ft plot of Ni/DOBDC pellet (R = 0.57 mm) at 0.1bar of CO_2 in helium, 38 °C, 5, 10, 20, 30, 45 cc/min and the blank response at 30, 45 cc/min

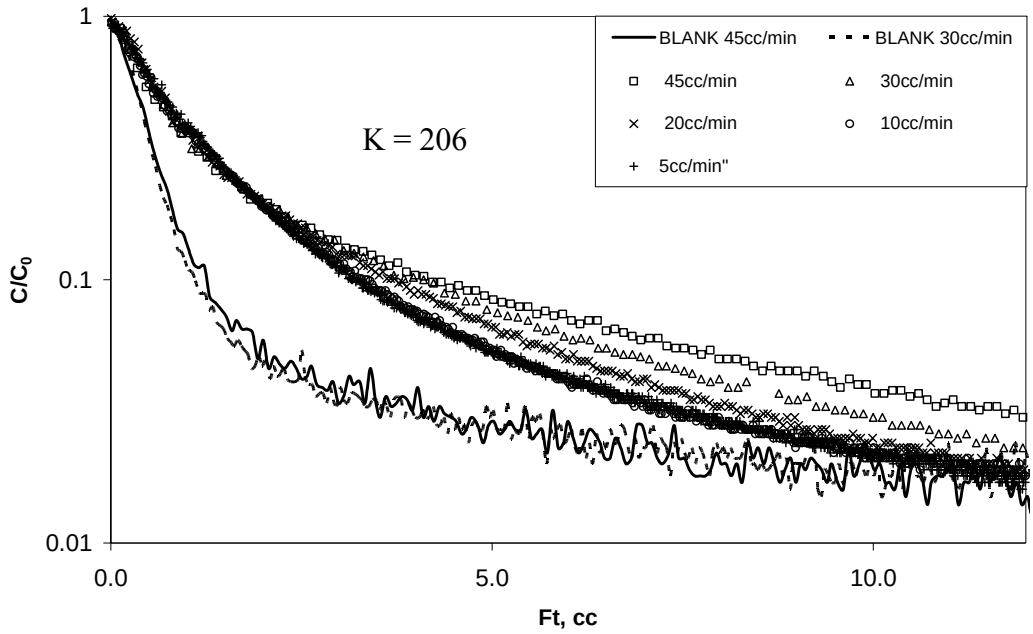

Figure 8. Experimental Ft plot of Ni/DOBDC pellet (R = 0.79 mm) at 0.1bar of CO_2 in helium, 38 °C, 5, 10, 20, 30, 45 cc/min and the blank response at 30, 45 cc/min

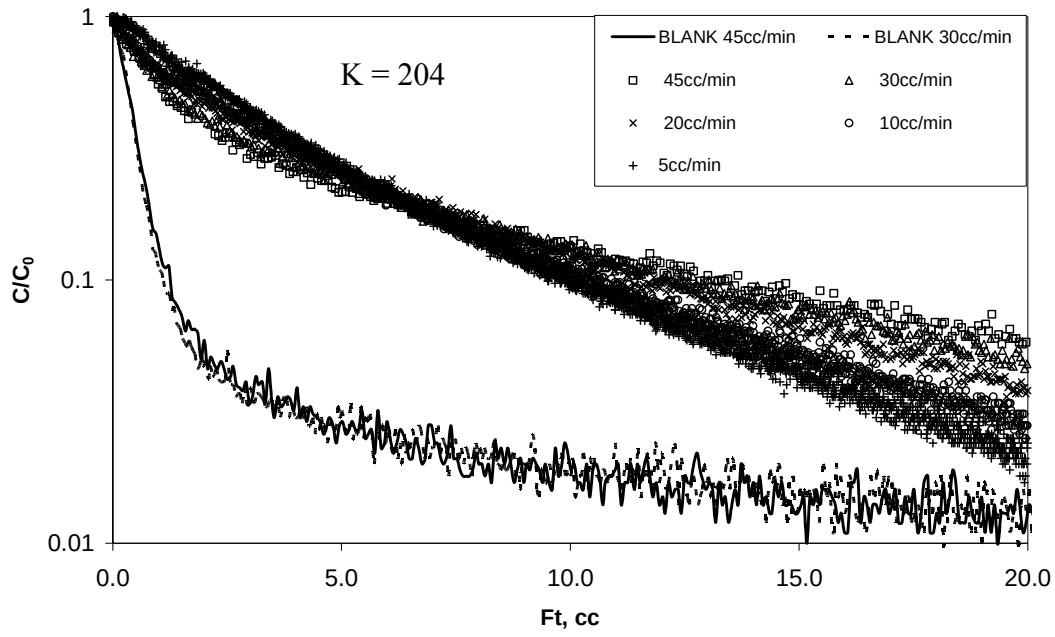

Figure 9. Experimental Ft plot of Ni/DOBDC pellet (R = 1.19 mm) at 0.1bar of CO_2 in helium, 38 °C, 5, 10, 20, 30, 45 cc/min and the blank response at 30, 45 cc/min.

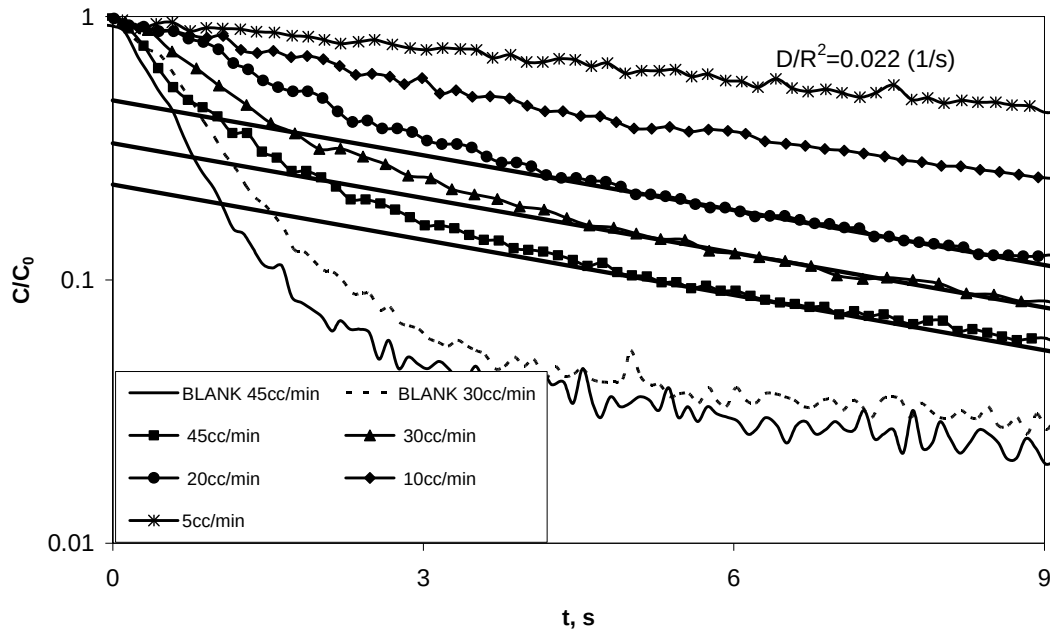

Figure 10. **Experimental ZLC response curves of Ni/DOBDC pellet (R = 0.79 mm) at 0.1bar of CO_2 in helium, 38 °C, 5, 10, 20, 30, 45 cc/min and the blank response at 30, 45 cc/min.**

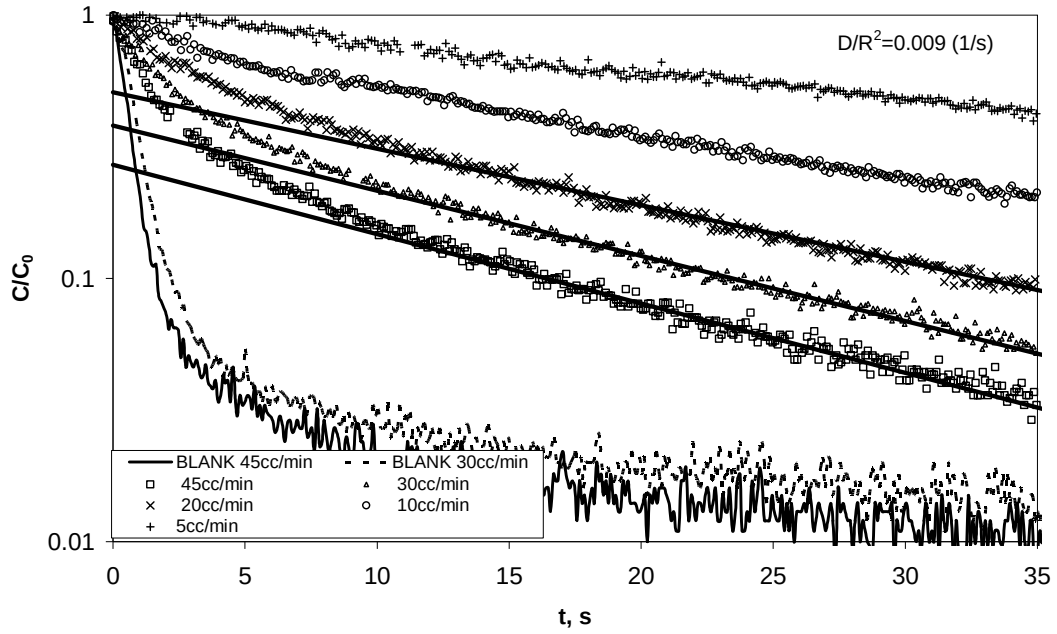

Figure 11. Experimental ZLC response curves of Ni/DOBDC pellet (R = 1.19 mm) at 0.1bar of CO_2 in helium, 38 °C, 5, 10, 20, 30, 45 cc/min and the blank response at 30, 45 cc/min

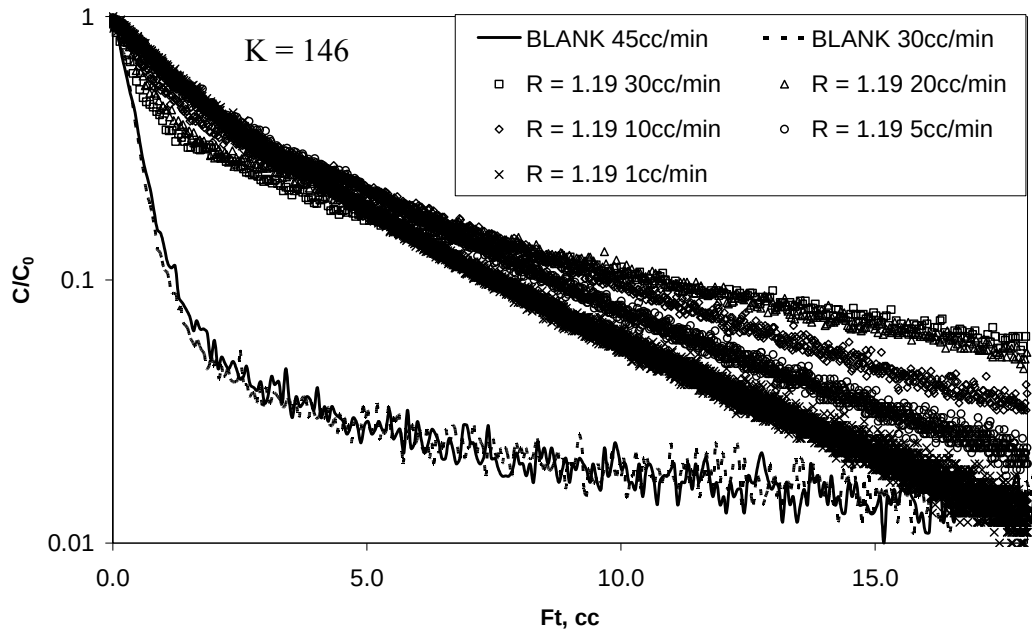

Figure 12. Experimental Ft plot of Ni/DOBDC pellet (R = 1.19 mm) at 0.1bar of CO_2 in nitrogen, 38 °C, 10, 20, 30, 45 cc/min and the blank response at 30, 45 cc/min

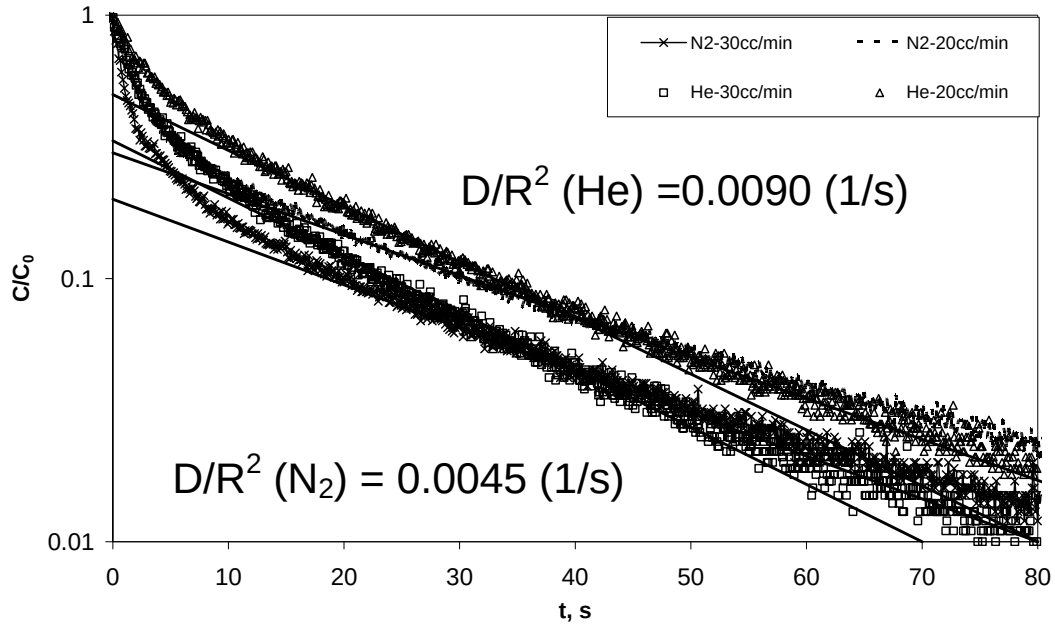

Figure 13. Comparison of experimental ZLC response curves of Ni/DOBDC pellet (R = 1.19 mm) at 0.1bar of CO_2 in two different purge gas (N_2 and He), 38 °C, 20 and 30 cc/min

Table 1. Dimensions measured by image analysis tool (GIMP) of the fragments and the calculated equivalent radius.

Fragments	Mass of sample (mg)	Width (mm)	Length (mm)	Height (mm)	Surface Area (mm^2)	Volume (mm^3)	Equivalent Radius (mm)
b	8.8	2.0	4.2	1.9	40.4	16.0	1.19
c	2.7	1.8	2.0	1.2	16.3	4.3	0.79
d	1.5	1.0	1.4	1.0	7.6	1.4	0.57

Table 2. Summary of Parameters from the ZLC Analysis

Equivalent Radius (mm)	**Carrier Gas**	**K**	**D_p/R^2 (1/s)**	**D_m of CO_2 (m^2/s)**	**ε_P**	**τ**
0.79	Helium	205	0.022	$0.625*10^{-4}$	0.21	4.7
1.19	Helium	204	0.009	$0.625*10^{-4}$	0.20	4.9
1.19	Nitrogen	146	0.045	$0.164*10^{-4}$	0.24	4.2

For Table of Contents Only